



# Friction and wear characteristics of bismuth selenide topological insulator

Utku Uzun<sup>a,\*</sup>, Caterina Lamuta<sup>b</sup>, Mehmet Yetmez<sup>c</sup>

<sup>a</sup> Department of Aerospace Engineering, Tarsus University, Tarsus, Mersin 33400, Turkey

<sup>b</sup> Department of Mechanical Engineering, University of Iowa, Iowa City, IA 52242, USA

<sup>c</sup> Department of Mechanical Engineering, Zonguldak Bülent Ecevit University, Zonguldak 67100, Turkey

## ARTICLE INFO

### Keywords:

Bi<sub>2</sub>Se<sub>3</sub>  
Crystal growth  
Superconductors  
Scratch  
Mechanical properties

## ABSTRACT

Single crystal Bi<sub>2</sub>Se<sub>3</sub> was grown using the novel Bridgeman-Stockbarger method. Surface characteristics in terms of wear rate (*W*), wear coefficient (*K*), coefficient of friction (*COF*), and strain hardening exponent (*n*) were investigated using nanoindentation and nano scratch techniques. Our results revealed that the remarkable wear properties of single-crystal Bi<sub>2</sub>Se<sub>3</sub> are promising for nanoscale design of topological insulators.

## 1. Introduction

In recent years, the demand for high-speed data processing has emerged because of the spread of digitalization and the increase in data volume. Therefore, new materials are needed to transmit these data faster as datasets grow. Topological insulators (TIs) are a new group of materials that can transmit data faster thanks to their unique spin-orbit coupling system [1]. Bismuth selenide (Bi<sub>2</sub>Se<sub>3</sub>), a traditional semiconductor, has rapidly increased in popularity in recent years due to the discovery of TI properties that provide exceptional conductivity [2]. Its superior conduction properties make it an essential potential candidate for quantum computers [3] and optoelectronics [4]. However, the remarkable advances in understanding the electronic properties of Bi<sub>2</sub>Se<sub>3</sub>-based materials contrast with the understanding of the mechanical properties of Bi<sub>2</sub>Se<sub>3</sub>. An incomplete understanding of the material's mechanical properties may pose a problem for the design and limit its use in new high-tech applications. To date, the mechanical properties of Bi<sub>2</sub>Se<sub>3</sub>, such as hardness, Young's modulus, and fracture toughness [5], have been comprehensively examined. However, the tribological properties of the material are still lacking, which is of great importance because the superior electrical properties are strongly dependent on surface integrity and crystallographic quality [6].

In this study, the wear and friction properties of single-crystal Bi<sub>2</sub>Se<sub>3</sub> in terms of wear volume, wear rate, and coefficient of friction were analyzed for the first time using the nanoscratch technique. In addition, the strain hardening exponent was evaluated with a novel method based on pile-up width using nanoindentation tests. This study aims to

understand the wear behavior of single-crystal Bi<sub>2</sub>Se<sub>3</sub> for design purposes, whose excellent electronic properties are still being investigated.

## 2. Experimental

Bulk Bi<sub>2</sub>Se<sub>3</sub> single-crystal was grown using the Bridgeman-Stockbarger method. To start the crystal growth process, polycrystalline Bi and Se samples having a high purity ratio (99.999%) were placed into a conical-based quartz crucible and sealed under a vacuum. The crucible was heated at a constant temperature (1050 K) for 12 h before the melt was transferred to the cool zone (900 K). The transfer speed was set to 1 mm/h to obtain a good-quality crystal.

Nano scratch tests were performed in either constant or ramping load modes. In the case of continuous load mode, the samples were penetrated until the scratch load was achieved and then scratched along the scratch distance. In the ramping load mode, the load was continuously increased along the scratch distance until the scratch load was reached. Tests were conducted from 500 μN to 2500 μN with 500 μN intervals. A standard Berkovich tip with a tip radius of 82 nm and a half-angle  $\theta = 65.27^\circ$  was used in all tests using the Hystriion Triboindenter (TI-950). Scratch speed and scratch distance were set to 0.2 μm/s and 10 μm for all tests. To evaluate the stress hardening exponent (*n*), five indentation loads from 5000 μN to 9000 μN with 1000 μN intervals were applied to the sample's surface. Each testing condition was repeated five times to ensure reliability.

\* Corresponding author.

E-mail address: [utkuuzun@tarsus.edu.tr](mailto:utkuuzun@tarsus.edu.tr) (U. Uzun).

<https://doi.org/10.1016/j.matlet.2023.134402>

Received 30 January 2023; Received in revised form 23 March 2023; Accepted 17 April 2023

Available online 23 April 2023

0167-577X/© 2023 Elsevier B.V. All rights reserved.

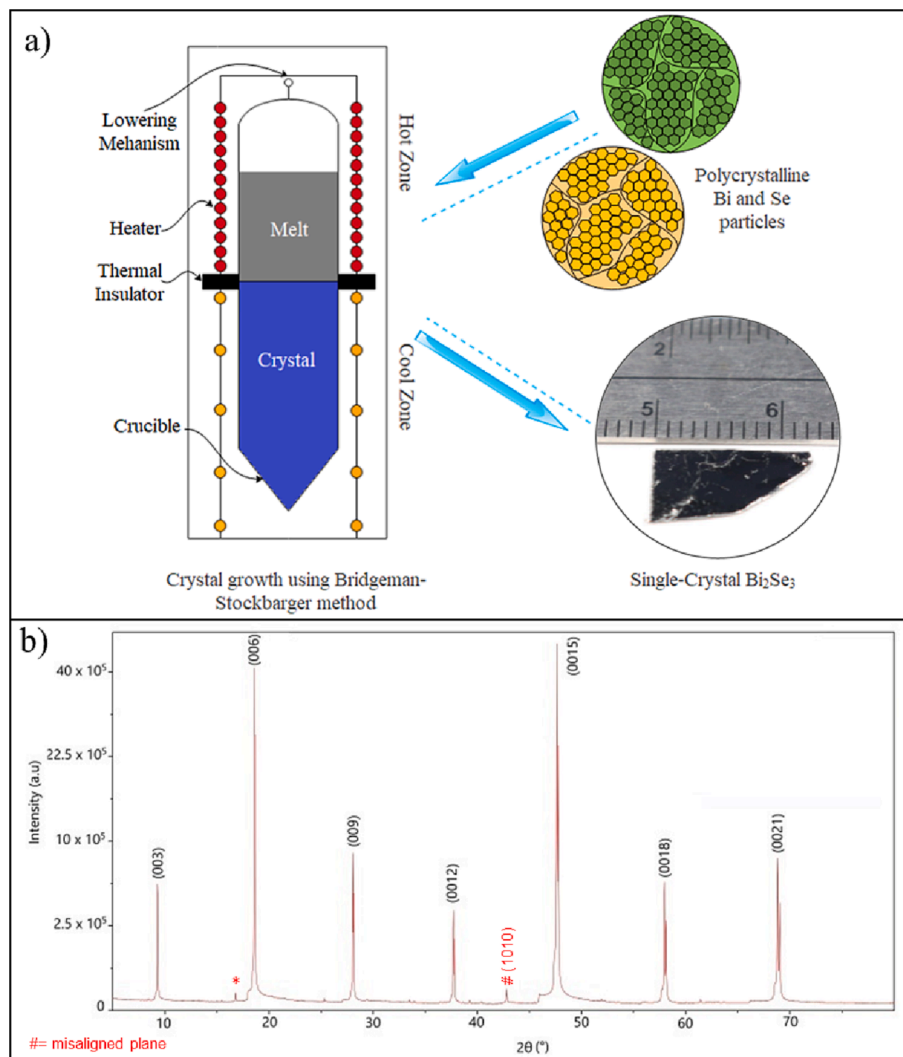


Fig. 1. (a) Schematic representation of single crystal growth of  $\text{Bi}_2\text{Se}_3$  (b) XRD patterns of the grown sample.

### 3. Results & discussion

The crystal growth process and X-Ray diffraction (XRD) patterns are illustrated in Fig. 1(a) and 1(b), respectively. Highly indexed peaks with (001) directions reflect the single crystalline structure of the sample. It is also observed that there are small peaks around  $17^\circ$  and  $43.5^\circ$ . The first of these peaks is unidentified, and the second is due to a misaligned  $\text{Bi}_2\text{Se}_3$  plane. Fig. 2(a) shows the normal displacement and normal force versus lateral displacement at loads ramping from 0 to  $1500 \mu\text{N}$ . The normal displacement measured during testing increased linearly with the increase in lateral displacement, eventually reaching  $2607 \text{ nm}$ , while the post-scratch depth of the compound slightly increased along with the scratch distance and was recorded as  $166.04 \text{ nm}$  at its maximum. In other words, the compound regained  $93.63 \pm 1.5\%$  of its initial volume after being subjected to plastic deformation due to scratching. A linear increase in the normal force followed by a linear increase in instantaneous scratch depth suggests the tip encountered a slight resistance. A side view of the surface at ramp load increasing from 0 to  $1500 \mu\text{N}$  is presented as an inset to Fig. 2(b), and plastic deformation is present with the onset of the normal force.

Fig. 2(b) illustrates the COF versus normal load. COF tends to stabilize after the initial rapid decline as the normal load increases. The rapid initial decrease could be attributed to adhesive forces that significantly increase the frictional forces between the tip and the specimen. COF values are even higher than one in this test stage because normal

force is too low to produce plastic deformation. In the steady-state phase, some fluctuations and spikes are visible. This is due to the stick-and-slip motion within the specimen. In the stick phase, the movement of the indenter tip is constrained by surrounding  $\text{Bi}_2\text{Se}_3$  piles. Therefore, the lateral force increases due to the resistance of piles. As the normal force increases to the critical point, the lateral force increases too and starts to push the piles in the scratch direction, and the slip phase takes place. Lateral force drops sharply in the slip phase causing spikes in the COF-Normal load graph, which can be seen in Fig. 2(b).

Fig. 3(a), 3(b), and 3(c) represent the three-dimensional and side views of the scratch trace of single crystal  $\text{Bi}_2\text{Se}_3$  under  $1500 \mu\text{N}$  constant load test, respectively. From Fig. 3(a), it was observed that a V-shaped groove was formed on the sample surface due to the pyramidal shape of the Berkovich tip, and accumulation of pile-ups is visible on the surfaces on both sides of the groove. The large pile-ups are due to the material pile movement towards the surface due to the initial immersion of the penetrating tip and plowing. Irregular stripes consisting of slip lines appear on the groove walls due to the stick and slip motion of the scratching process. Cross-slip events on groove walls where dislocations move from one slip line to another, suggesting that the dislocations are strong enough to overcome plane obstacles by changing the slip lines. Fig. 3(b) and 3(c) present the side views of the scratch trace in the x-y and y-z directions, respectively. As can be seen, the residual scratch depth is recorded as  $198.05 \text{ nm}$  along the scratch length.

Pile-ups around the scratch tracks indicate the material's ductility,

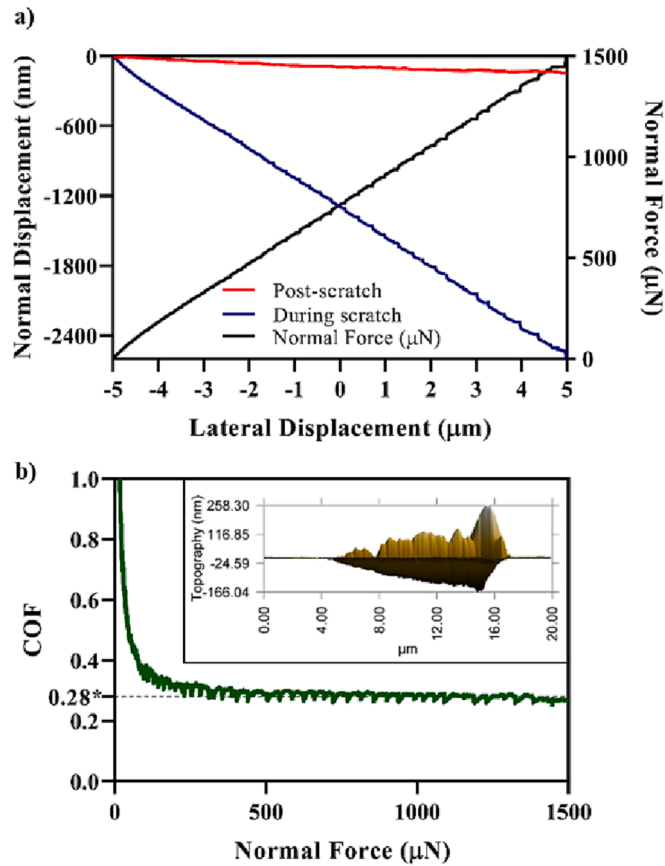


Fig. 2. (a) Surface profiles of single-crystal bismuth selenide (b) COF as a function of normal load.

thus its formability. To examine these pile-ups, strain hardening was measured. To assess the strain hardening of single-crystal Bi<sub>2</sub>Se<sub>3</sub>, a novel method based on the ratio of pile heights proposed by Das et al. [7] is used. According to the method, the strain hardening exponent, *n*, is calculated using the known radius of a cono-spherical tip and the radius of pile-up around the imprint using the following equation;

$$c^2 = \frac{a^2}{a^{*2}} = \frac{5(2 - n)}{2(4 + n)} \quad (4)$$

where *c* is a constant, *a* is the actual contact (pile-up) radius, and *a\** is the ideal contact (without pile-up) radius. According to the strain hardening coefficient classification, the value of *n* varies between 0 and 1, values close to 1 indicate that the material has predominantly elastic behavior, and values close to 0 indicate that the material has more plastic behavior. Using the above equation, *n* = 0.61 ± 0.07 was found for single-crystal Bi<sub>2</sub>Se<sub>3</sub>, reflecting the elastoplastic behavior.

Fig. 3(d) and 3(e) show that prominent pile-ups are generated around the imprint due to 8000 μN normal load. The normal displacement of the imprint is measured as 127.96 nm, whereas the instantaneous scratch depth is recorded as 670.38 nm for the same experiment. We can confirm that the material regains most of its initial volume after deformation. The generation of large pile-ups and the high recovery rate of initial volume indicates that the single-crystal Bi<sub>2</sub>Se<sub>3</sub> possesses both ductile and elastic properties to a large extent.

Wear rate (*W*) is a good indicator of the materials' scratch resistance and defined as volume loss (*V*) per distance (*L*). *V* can be calculated as follows;

$$V = \int_{-l/2}^{l/2} A(x) dx \quad (1)$$

here *A* is the cross-sectional area of the trace. Archard's equation [8] for dry wear can be employed as follows;

$$V = \frac{KF_n L}{H} \quad (2)$$

Here *K* represents the wear coefficient which indicates the probability of material removal, *F<sub>n</sub>* is the normal force applied on the surface, and *H* is the hardness. Therefore, *W* can be expressed as;

$$W = \frac{KF_n}{H} \quad (3)$$

In Fig. 4(a), the removed volume is plotted against the scratch length at loads varying from 500 μN to 2500 μN. It can be seen from the figure that the removed volume increased linearly as the scratch length increased for all loadings. To find the wear rates, the slope of the *V-L* curves from Fig. 4(a) was taken, and results are presented against the ratio of applied normal force versus hardness in Fig. 4(b). *K* is found to be 0.0623 by the slope of the curve in Fig. 4(b) according to Eq. (3).

#### 4. Conclusions

In summary, Bi<sub>2</sub>Se<sub>3</sub> topological insulator grown with the Bridgeman-Stockbarger technique recovers most of its original volume once

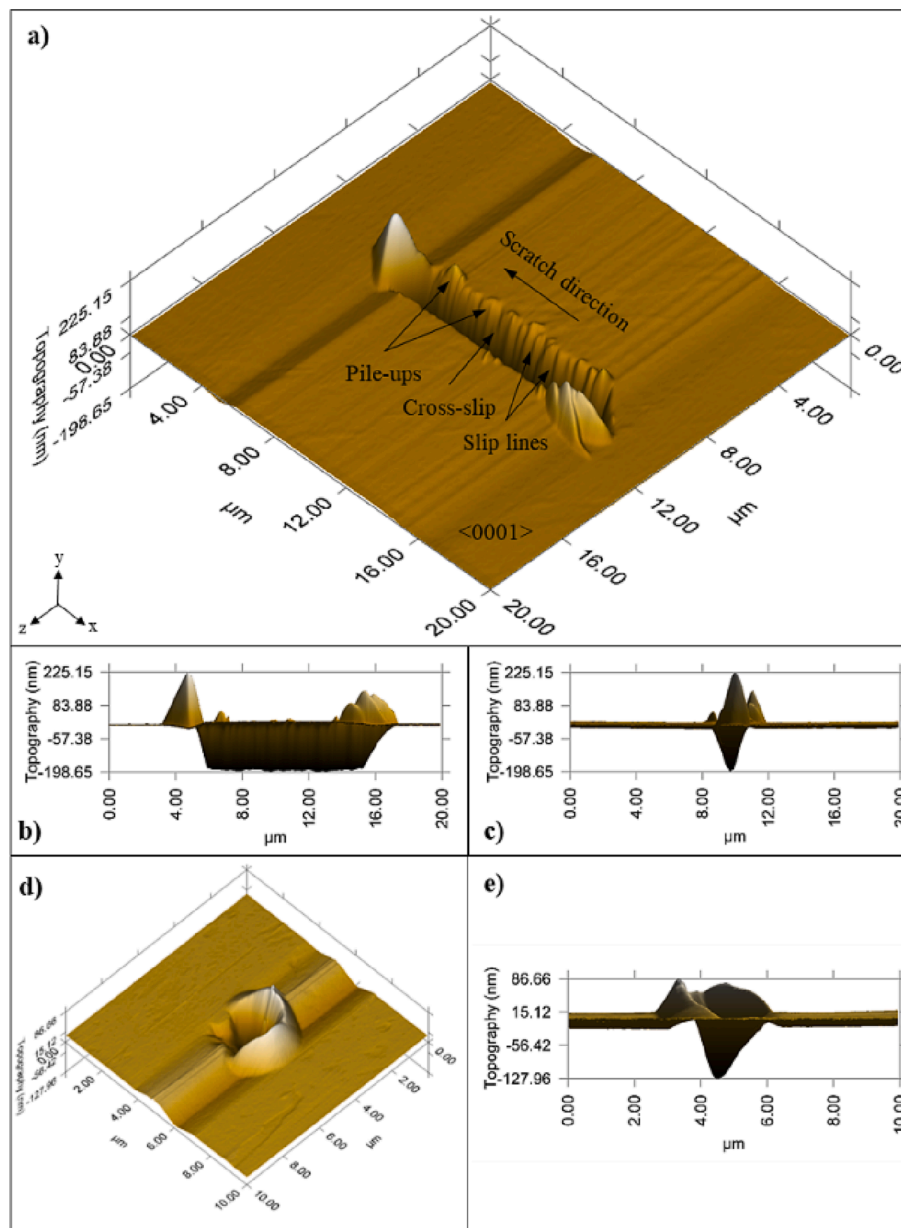


Fig. 3. SPM images of the (a-c) post-scratch surface at 150  $\mu\text{N}$  and (d-e) indentation imprint at 8000  $\mu\text{N}$ .

subjected to abrasion, as suggested by the volume recovery rate of 93.63%. COF is found to be 0.28, which is very close to that of GaN ( $\approx 0.27$ ) [9].  $K$  is found as 0.0623.  $n$  is found as  $0.61 \pm 0.07$ , slightly higher than polycrystalline Cu (0.456) [10]. Based on the results obtained in this work, we can conclude that single-crystal  $\text{Bi}_2\text{Se}_3$  has competitive friction and wear properties in addition to its superior electronic properties, when compared to conventional flexible electronics. Our results revealed that these superior wear resistance properties of single-crystal  $\text{Bi}_2\text{Se}_3$  can promote its use in future electronic systems.

#### CRediT authorship contribution statement

**Utku Uzun:** Conceptualization, Methodology, Writing – original

draft, Investigation, Visualization, Methodology, Validation. **Caterina Lamuta:** Writing – review & editing, Resources, Supervision. **Mehmet Yetmez:** Resources, Supervision.

#### Declaration of Competing Interest

The authors declare the following financial interests/personal relationships which may be considered as potential competing interests: Utku Uzun reports financial support was provided by The Scientific and Technological Research Council of Turkey.

#### Data availability

Data will be made available on request.

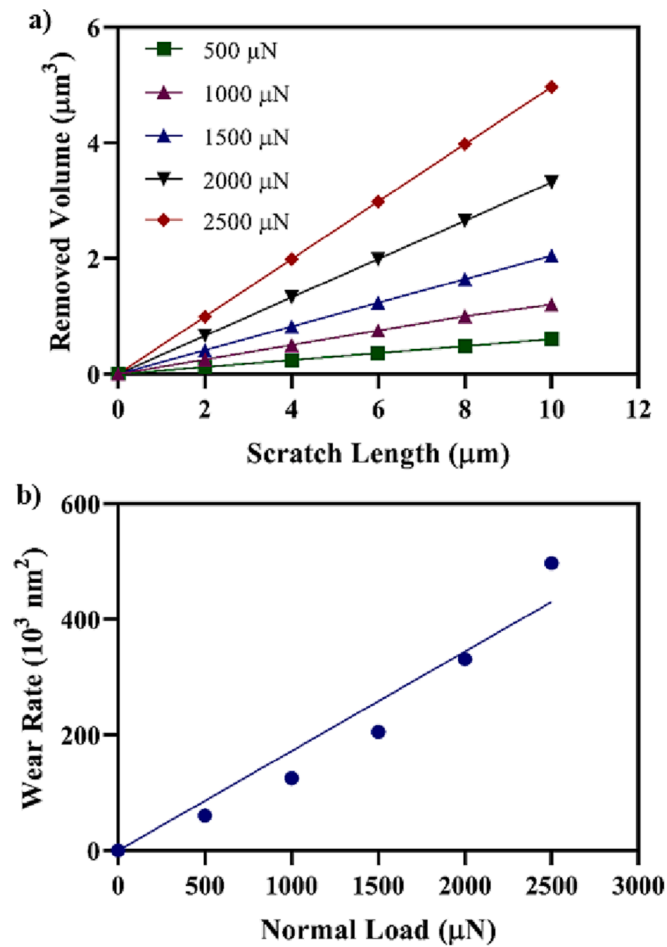


Fig. 4. (a). Scratch volume against scratch length for five different normal loads (b) wear rate against normal load for single-crystal  $\text{Bi}_2\text{Se}_3$ .

## References

- [1] C.L. Kane, E.J. Mele, Phys. Rev. Lett. 95 (146802) (2005) 3–6, <https://doi.org/10.1103/PhysRevLett.95.146802>.
- [2] W. Zhou, H. Zhu, J.A. Yarmoff, Phys. Rev. B 94 (19) (2016) 1–10, <https://doi.org/10.1103/PhysRevB.94.195408>.
- [3] L.A. Jauregui, M.T. Pettes, L.P. Rokhinson, L. Shi, Y.P. Chen, Nat. Nanotechnol. 11 (4) (2016) 345–351, <https://doi.org/10.1038/nnano.2015.293>.
- [4] H. Xie, et al., Small 12 (30) (2016) 4136–4145, <https://doi.org/10.1002/sml.201601050>.
- [5] U. Uzun, M. Yetmez, N. Akinci, Micro Nano Lett. 16 (3) (2021) 203–212, <https://doi.org/10.1049/mna2.12025>.
- [6] J.J. Cha, K.J. Koski, Y. Cui, Phys. Status Solidi – Rapid Res. Lett. 7 (1–2) (2013) 15–25, <https://doi.org/10.1002/pssr.201206393>.
- [7] G. Das, S. Ghosh, S. Ghosh, R.N. Ghosh, Mater. Sci. Eng. A 408 (1–2) (2005) 158–164, <https://doi.org/10.1016/j.msea.2005.07.026>.
- [8] J.F. Archard, J. Appl. Phys. 24 (8) (1953) 981–988, <https://doi.org/10.1063/1.1721448>.
- [9] G. Zeng, C.K. Tan, N. Tansu, B.A. Krick, Appl. Phys. Lett. 109 (5) (2016) pp, <https://doi.org/10.1063/1.4960375>.
- [10] B.M. Kim, C.J. Lee, J.M. Lee, J. Mech. Sci. Technol. 24 (1) (2010) 73–76, <https://doi.org/10.1007/s12206-009-1115-8>.